



# Mutual promotion effect between aerosol particle liquid water and nitrate formation lead to severe nitrate-dominated particulate matter pollution and low visibility

Yu Wang<sup>1,2,a</sup>, Ying Chen<sup>3,a</sup>, Zhijun Wu<sup>1,4,5,\*</sup>, Dongjie Shang<sup>1</sup>, Yuxuan Bian<sup>6</sup>, Zhuofei Du<sup>1,b</sup>, Sebastian  
5 H. Schmitt<sup>4,7,c</sup>, Rong Su<sup>1,d</sup>, Georgios I. Gkatzelis<sup>4,7,e,f</sup>, Patrick Schlag<sup>4,7,g</sup>, Thorsten Hohaus<sup>4,7</sup>, Aristeidis  
Voliotis<sup>2</sup>, Keding Lu<sup>1,4,5</sup>, Limin Zeng<sup>1,4</sup>, Chunsheng Zhao<sup>8</sup>, Rami Alfarra<sup>2,9</sup>, Gordon McFiggans<sup>2</sup>, Alfred  
Wiedensohler<sup>10</sup>, Astrid Kiendler-Scharr<sup>4,7</sup>, Yuanhang Zhang<sup>1,4,5</sup>, Min Hu<sup>1,4,5</sup>

<sup>1</sup>State Key Joint Laboratory of Environmental Simulation and Pollution Control, College of Environmental  
Sciences and Engineering, Peking University, Beijing 100871, China

10 <sup>2</sup>Centre for Atmospheric Science, School of Earth and Environmental Sciences, The University of  
Manchester, Manchester M13 9PL, UK

<sup>3</sup>Lancaster Environment Centre, Lancaster University, Lancaster, LA1 4YQ, UK

<sup>4</sup>International Joint Laboratory for Regional Pollution Control, 52425 Jülich, Germany, and Beijing 100871,  
China

15 <sup>5</sup>Collaborative Innovation Center of Atmospheric Environment and Equipment Technology, Nanjing  
University of Information Science and Technology, Nanjing 210044, China

<sup>6</sup>State Key Laboratory of Severe Weather, Chinese Academy of Meteorological Sciences, Beijing, 100081,  
China

20 <sup>7</sup>Institute for Energy and Climate Research, IEK-8: Troposphere, Forschungszentrum Jülich, 52425 Jülich,  
Germany

<sup>8</sup>Department of Atmospheric and Oceanic Sciences, School of Physics, Peking University, Beijing 100871,  
China

<sup>9</sup>National Centre for Atmospheric Science, School of Earth and Environmental Sciences, The University of  
Manchester, Manchester, M13 9PL, UK

25 <sup>10</sup>Leibniz Institute for Tropospheric Research, 04318 Leipzig, Germany

<sup>a</sup>These authors contribute equally to this work

<sup>b</sup>Now at Center for Urban Transport Emission Research & State Environmental Protection Key Laboratory  
of Urban Ambient Air Particulate Matter Pollution Prevention and Control, College of Environmental  
30 Science and Engineering, Nankai University, Tianjin, 300071, China

<sup>c</sup>Now at TSI GmbH, 52068 Aachen, Germany

<sup>d</sup>Now at Guangdong Science and Technology Monitoring and Research Center, Guangzhou 510033, China

<sup>e</sup>Now at NOAA Earth Systems Research Laboratory, Boulder, Colorado 80305, United States

35 <sup>f</sup>Now at Cooperative Institute for Research in Environmental Sciences, Boulder, Colorado 80309, United  
States

<sup>g</sup>Now at Shimadzu Deutschland GmbH, 47269 Duisburg, Germany

Correspondence to: Zhijun Wu ([zhijunwu@pku.edu.cn](mailto:zhijunwu@pku.edu.cn))



**Abstract.** As has been the case in North America and Western Europe, the SO<sub>2</sub> emissions substantially  
40 reduced in North China Plain (NCP) in recent years. A dichotomy of reductions in SO<sub>2</sub> and NO<sub>x</sub>  
concentrations result in the frequent occurrences of nitrate (pNO<sub>3</sub><sup>-</sup>)-dominated particulate matter  
pollution over NCP. In this study, we observed a polluted episode with the nitrate mass fraction in non-  
refractory PM<sub>1</sub> (NR-PM<sub>1</sub>) up to 44% during wintertime in Beijing. Based on this typical pNO<sub>3</sub><sup>-</sup>-  
dominated haze event, the linkage between aerosol water uptake and pNO<sub>3</sub><sup>-</sup> formation, further  
45 impacting on visibility degradation, have been investigated based on field observations and theoretical  
calculations. During haze development, as ambient relative humidity (RH) increased from ~10% up to  
70%, the aerosol particle liquid water increased from ~1 μg/m<sup>3</sup> at the beginning to ~75 μg/m<sup>3</sup> at the  
fully-developed haze period. Without considering the water uptake, the particle surface area and the  
volume concentrations increased by a factor of 4.1 and 4.8, respectively, during the development of  
50 haze event. Taking water uptake into account, the wet particle surface area and volume concentrations  
enhanced by a factor of 4.7 and 5.8, respectively. As a consequence, the hygroscopic growth of particles  
facilitated the condensational loss of dinitrogen pentoxide (N<sub>2</sub>O<sub>5</sub>) and nitric acid (HNO<sub>3</sub>) to particles  
contributing pNO<sub>3</sub><sup>-</sup>. From the beginning to the fully-developed haze, the condensational loss of N<sub>2</sub>O<sub>5</sub>  
increased by a factor of 20 when only considering aerosol surface area and volume of dry particles,  
55 while increasing by a factor of 25 considering extra surface area and volume due to water uptake.  
Similarly, the condensational loss of HNO<sub>3</sub> increased by a factor of 2.7~2.9 and 3.1~3.5 for dry and wet  
aerosol surface area and volume from the beginning to the fully-developed haze period. Above results  
demonstrated that the pNO<sub>3</sub><sup>-</sup> formation is further enhanced by aerosol water uptake with elevated  
ambient RH during haze development, in turn, facilitating the aerosol taking up water due to the



60 hygroscopicity of nitrate salt. Such mutual promotion effect between aerosol particle liquid water and  
nitrate formation can rapidly degrade air quality and halve visibility within one day. Reduction of  
nitrogen-containing gaseous precursors, e.g., by control of traffic emissions, is essential in mitigating  
severe haze events in NCP.

65

70

75



## 1 Introduction

80 Aerosol particle hygroscopicity plays an important role in air quality deterioration and cloud formation  
(Yu, 2009; Fitzgerald, 1973; Kreidenweis and Asa-Awuku, 2014; Wang and Chen, 2019; McFiggans et  
al., 2006) and can also directly influence aerosol measurements (Chen et al., 2018a). In atmospheric  
environments influenced by anthropogenic activities, particulate secondary inorganic compounds are  
often dominated by ammonium sulfate ((NH<sub>4</sub>)<sub>2</sub>SO<sub>4</sub>) and ammonium nitrate (NH<sub>4</sub>NO<sub>3</sub>) (Heintzenberg,  
85 1989), which originate from the oxidation of sulfur dioxide (SO<sub>2</sub>) and nitrogen oxides (NO<sub>x</sub>) via well-  
established chemical pathways (Calvert et al., 1985). The abundance of secondary inorganic  
components is one of the most important factors determining particle hygroscopicity (Swietlicki et al.,  
2008), thereby governing the aerosol liquid water content under ambient moist conditions. Increased  
aerosol particle liquid water could accelerate secondary inorganic and organic aerosol formation by  
90 decreasing the kinetic limitation of mass transfer of gaseous precursors and providing more medium for  
multiphase reactions (Mozurkewich and Calvert, 1988; Cheng et al., 2016; Wang et al., 2016; Ervens et  
al., 2011; Kolb et al., 2010).

Sulfuric acid (H<sub>2</sub>SO<sub>4</sub>) is formed from the oxidation of SO<sub>2</sub> via gaseous and multiphase reactions. H<sub>2</sub>SO<sub>4</sub>  
is subsequently fully or partly neutralized by gaseous NH<sub>3</sub> taken up on particles, resulting in the  
95 formation of (NH<sub>4</sub>)<sub>2</sub>SO<sub>4</sub> and / or NH<sub>4</sub>HSO<sub>4</sub>. Any remaining NH<sub>3</sub> is available to neutralize HNO<sub>3</sub> to  
form particulate NH<sub>4</sub>NO<sub>3</sub> (Seinfeld. and Pandis., 2006) (and further excess NH<sub>3</sub> can neutralize any  
available HCl to form particulate NH<sub>4</sub>Cl). Over the past several decades, substantial efforts have  
reduced emissions of both SO<sub>2</sub> and NO<sub>x</sub> improving the local and regional air quality all over the world.



For example,  $\text{SO}_2$  and  $\text{NO}_x$  emissions were reduced by 82% and 54% in the majority of European  
100 Environment Agency member countries between 1990 and 2016 ([https://www.eea.europa.eu/data-and-](https://www.eea.europa.eu/data-and-maps/indicators/main-anthropogenic-air-pollutant-emissions/assessment-4)  
[maps/indicators/main-anthropogenic-air-pollutant-emissions/assessment-4](https://www.eea.europa.eu/data-and-maps/indicators/main-anthropogenic-air-pollutant-emissions/assessment-4)). In consequence, an  
increasing trend of  $\text{NO}_3^-/\text{SO}_4^{2-}$  molar ratio was observed in long-term measurements at Leipzig,  
Germany (Spindler et al., 2004) and at some other European sites from the European Monitoring and  
Evaluation Programme (EMEP) (Putaud et al., 2004). In recent years, China has also managed to reduce  
105  $\text{SO}_2$  emissions by 75% since 2007 (Li et al., 2017a), whereas  $\text{NO}_x$  emissions declined only by ~10%  
between 2011 and 2015 (de Foy et al., 2016). Similar with European countries, the dominant inorganic  
component in fine aerosol particles has switched from sulfate to nitrate in the recent years (Sun et al.,  
2015;Hu et al., 2017;Hu et al., 2016;Wu et al., 2018;Guo et al., 2014;Huang et al., 2014;Huang et al.,  
2010;Ge et al., 2017;Xu et al., 2019a;Xie et al., 2019;Li et al., 2018). Field measurements show that  
110 annually averaged  $\text{NO}_3^-/\text{SO}_4^{2-}$  molar ratio of NR- $\text{PM}_{10}$  (non-refractory  $\text{PM}_{10}$ ) in 2012 (1.3~1.8) (Sun et  
al., 2015) has significantly increased compared to that in 2008 (0.9~1.5) (Zhang et al., 2013).  
Comparably, the  $\text{NO}_3^-/\text{SO}_4^{2-}$  molar ratio of  $\text{PM}_{2.5}$  increased substantially, from 1.5 before 2013 to 3.33  
in 2017 (Xu et al., 2019a). Model simulations have also shown that the simulated annual mass  
concentration of nitrate and its mass fraction in secondary inorganic components over North China  
115 increased by 17~19% and 7% respectively, while the sulfate mass and fraction decreased by 10~19%  
and 6% between 2006 and 2015 under the assumption of constant  $\text{NH}_3$  emissions (Wang et al., 2013).  
However,  $\text{NH}_3$  emissions have been observed by satellites to increase by ~30% from 2008 to 2016 over  
the North China Plain (NCP) (Liu et al., 2018), further increasing the potential for nitrate formation  
(Wang et al., 2013).



120 Over the NCP region, heavy haze events are typically associated with enhanced ambient RH levels. This leads to an increased aerosol liquid water content (Wu et al., 2018), which will influence the particulate nitrate formation by changing the reactive uptake of precursors and the thermodynamic equilibrium of ammonium nitrate (Cheng et al., 2016; Wang et al., 2016; Wang et al., 2017; Yun et al., 2018; Yue et al., 2019). To date, few studies reported aerosol liquid water content over NCP region  
125 (Wang et al., 2018; Bian et al., 2014; Cheng et al., 2016; Wu et al., 2018). However, the observational and theoretical analysis of the relationship between particulate nitrate formation and associated liquid water during haze events in China has been infrequently reported (Wu et al., 2018).

In this study, a self-amplification effect between particulate nitrate and liquid water is demonstrated by examining a nitrate-dominated fine particle Beijing pollution episode. The facilitation of particulate  
130 nitrate formation by abundant liquid water is subsequently theoretically explored through the impacts of liquid water on thermodynamic equilibrium and heterogeneous reactions. Finally, the corresponding impacts on light extinction coefficient, and visibility degradation are estimated. These results improve our quantitative understanding of the development of haze events over the NCP and on formulating emission reduction strategies, as well as may also provide insights for other polluted regions.

## 135 **2 Measurements and Methods**

### **2.1 Location and instrumentation**

Measurements were conducted within the framework of the BEST-ONE (Beijing winter fine particle Study- Oxidation, Nucleation, and light Extinctions) field campaign from January 1 to March 5, 2016,



at the Huairou site (40.42°N, 116.69°E), located in a rural environment, north of Beijing, China.

140 Detailed information about the sampling site was described in Tan et al. (2018). A weather station (Met one Instrument Inc., USA) was performed to measure meteorological parameters (ambient RH, temperature, wind speed, wind direction) and detailed aerosol particle physical and chemical properties were recorded using a suite of state-of-the-science instrumentation. Hygroscopic growth factor (HGF) of sub-micrometer aerosol particles was measured using a Hygroscopicity-Tandem Differential

145 Mobility Analyzer (H-TDMA, TROPOS, Germany) (Wu et al., 2011; Massling et al., 2011; Wang et al., 2018; Wu et al., 2016; Liu et al., 1978) and data retrieval followed the TDMA<sub>inv</sub> method in Gysel et al. (2009). The hygroscopicity parameter ( $\kappa$ ) was estimated using by the  $\kappa$ -Köhler approach (Petters and Kreidenweis, 2007; Köhler, 1936). Size-resolved NR-PM<sub>1</sub> was recorded by an Aerodyne High-Resolution Time-of-Flight Aerosol Mass Spectrometry (HR-ToF-AMS, Aerodyne Research, Inc., USA)

150 (DeCarlo et al., 2006). Regular calibration procedures followed as reported in Jayne et al. (2000) and Jimenez et al. (2003) and composition dependent correction followed as in Middlebrook et al. (2012). Gaseous HNO<sub>3</sub> and NH<sub>3</sub> were measured using Gas-Aerosol Collector (GAC) coupled with Ion Chromatography (IC) (Dong et al., 2012). Mass concentration of equivalent black carbon in aerosol particles (Petzold et al., 2013) was recorded by Multi Angle Absorption Photometer (MAAP, Model

155 5012, Thermo Fisher Scientific, USA) with a laser wavelength of 670 nm (Petzold and Schönlinner, 2004). Furthermore, particle number size distribution (PNSD) in the size range of 3 nm~10  $\mu$ m was measured using a Mobility Particle Size Spectrometer (MPSS, Model 3776+3085 3775+3081, TSI, USA), following the recommendations described in Wiedensohler et al. (2012) and an Aerodynamic Particle Size Spectrometer (APS, Model 3021, TSI, USA) (Wu et al., 2008; Pfeifer et al., 2016).



160 Detailed description on H-TDMA, HR-ToF-AMS and GAC-IC can be found in the supporting information.

## 2.2 Estimation of aerosol particle liquid water

Given the absence of direct liquid water measurement, size-resolved liquid water was calculated using the corresponding HGFs measured at RH=90% (50, 100, 150, 250, 350 nm in stokes diameter), PNSD data (3 nm~10 μm) and meteorological parameters (RH, T), following the method proposed in Bian et al. (2014), referred to below as H-TDMA-derived liquid water. Briefly, the measured PNSD with 57 size bins were fitted using a four-mode lognormal distribution. The classification of four modes and the fitting results are shown in Table S1 and Figure S4. Good agreement between measured values and fitted PNSD was achieved, which indicates the reliability of the four-mode lognormal fitting method.

170 Based on four-mode lognormal fitting results, the particle number size distribution and number fractions of each mode can be obtained. It has been assumed that particles from the same mode have constant particle hygroscopicity ( $\kappa$ ). Under the assumption of constant particle hygroscopicity in each mode (shown in Table S1), the  $\kappa$  values for each mode ( $\kappa_1, \kappa_2, \kappa_3$ ) can be calculated by equation [1] from the known number fraction of fitted four modes and the  $\kappa$  values of measured particle size from H-TDMA

175 measurement.

$$\kappa = \sum_{i=1}^4 \kappa_i f_i \quad [1]$$

Here,  $\kappa_i$  and  $f_i$  represent the  $\kappa$  value and the particle number fraction of the  $i$  mode. Then, the calculated  $\kappa$  values for each mode and the derived number fraction of each size bin were used to obtain the  $\kappa$  distribution for each size bin. Figure S5 shows the comparison of calculated sized-resolved  $\kappa$





180 distribution and the  $\kappa$  measured by H-TDMA, the good agreement showed the reliability of the method. Then, based on  $\kappa$ -Köhler theory (Petters and Kreidenweis, 2007; Köhler, 1936), the size-resolved *HGF*s at ambient RH were calculated. Finally, liquid water of size-resolved particles can be derived by calculating the differentials between the dry and wet PNSD of aerosol particles in equation [2]:

$$\text{Liquid water} = \frac{\pi}{6} N_j D_{p,j}^3 \left( HGF(D_p, RH)^3 - 1 \right) * \rho_w \quad [2]$$

185 where  $j$  represents the bin number of measured PNSD,  $N_j$  and  $D_{p,j}$  represent the number concentration and the diameter of dry particles of the  $j^{\text{th}}$  bin, respectively, while, *HGF* and  $\rho_w$ , are the hygroscopic growth factor of aerosol particles and water density (1 g/cm<sup>3</sup>), respectively.

### 2.3 Condensation rate of trace gases

The condensation rate ( $k$ ) of trace gases (dinitrogen pentoxide, N<sub>2</sub>O<sub>5</sub> and nitric acid, HNO<sub>3</sub> in the  
 190 constrained conditions, referred as  $k_{\text{N}_2\text{O}_5}$  and  $k_{\text{HNO}_3}$  below) was calculated by the method of Schwartz (1986), shown in equation [3]. In order to illustrate the influences of the dry and wet PNSD due to water uptake on condensation rate of gases, the PNSD of the dry and wet particles (obtained by applying the *HGF* estimated from H-TDMA-derived liquid water method) were used.

$$k = \frac{4\pi}{3} \int_0^\infty \left( \frac{r^2}{3D_g} + \frac{4r}{3C_g v} \right)^{-1} r^3 \frac{dN}{d \log r} d \log r \quad [3]$$

195  $C_g = \sqrt{\frac{3RT}{M}} \quad [4]$

Where,  $r$  represents radius of the particles,  $D_g$  represents the binary diffusion coefficient evaluated following Maitland (1981) (1.18\*10<sup>-5</sup> m<sup>2</sup>/s).  $C_g$  is the kinetic velocity of the gas molecules, calculated in



equation [4]. Here,  $R$  and  $M$  are the ideal gas constant ( $8.314 \text{ kg.m}^2/\text{mol.K/s}^2$ ) and molar mass of the gas, respectively while  $T$  represents the ambient temperature.  $dN/d\log r$  is the number size distribution  
200 and  $\gamma$  is the uptake coefficient of the gas.

The uptake coefficient of  $\text{N}_2\text{O}_5$  was estimated following the method proposed in Chen et al. (2018b) and Chang et al. (2016) and references therein. The uptake suppression effect of  $\text{N}_2\text{O}_5$  due to the presence of secondary organic aerosol (SOA) was considered following the method in Anttila et al. (2006). Based on our source apportionment using Positive matrix factorization (SoFi tool, ME2, Francesco Canonaco, 205 PSI), two oxygenated organic aerosol factors (OOA), usually interpreted as SOA, and three primary organic aerosol factors (POA) were determined. The fraction of SOA in the total organic aerosol (OA) was 60%~90% during the observed period, which is quite consistent with the results of a previous study in Beijing (Huang et al., 2014). Hence, 75% was used as the ratio of SOA/OA in our model to calculate uptake coefficient of the  $\text{N}_2\text{O}_5$ , where the suppression effect of SOA on the uptake of  $\text{N}_2\text{O}_5$  was  
210 estimated following the work of Anttila et al. (2006). Additionally, the reaction of chloride with  $\text{N}_2\text{O}_5$  was not considered in this study due to its limited mass concentration (on average 5% of the  $\text{PM}_{10}$  mass concentration during the marked haze period), which might cause uncertainty in the  $k_{\text{N}_2\text{O}_5}$  calculation. The detailed information regarding the estimation  $\gamma_{\text{N}_2\text{O}_5}$  is given in Chen et al. (2018b). For the estimation of  $\gamma_{\text{HNO}_3}$ , it was reported that the  $\gamma_{\text{HNO}_3}$  on the solid and deliquesced inorganic compound  
215 such like sodium chloride were 0.01~0.03 (Fenter et al., 1994; Leu et al., 1995; Beichert and Finlayson-Pitts, 1996) and >0.2 (even 0.5) (Guimbaud et al., 2002; Abbatt and Waschewsky, 1998), respectively. Therefore,  $\gamma_{\text{HNO}_3}=0.01$  and  $\gamma_{\text{HNO}_3}=0.5$  are selected to calculate the lower and upper limit of condensation rate of  $\text{HNO}_3$  in the atmosphere.



## 2.4 Equilibrium of $\text{NH}_4\text{NO}_3$

220 The equilibrium dissociation constant of  $\text{NH}_4\text{NO}_3$  ( $K_p$ ) under dry conditions was calculated as a function of ambient temperature (Seinfeld. and Pandis., 2006) in the following equation [5].

$$\ln K_p = 84.6 - \frac{24220}{T} - 6.1 \ln \left( \frac{T}{298} \right) \quad [5]$$

Taking into account the associated liquid water, the equilibrium vapor pressure of  $\text{HNO}_3$  was calculated by employing the Extended-Aerosol Inorganic Model (E-AIM) Model II  $\text{H}^+ - \text{NH}_4^+ - \text{SO}_4^{2-} - \text{NO}_3^- - \text{H}_2\text{O}$  (Clegg et al., 1998) using HR-ToF-AMS data,  $\text{NH}_3$  from GAC-IC, and meteorological parameters (RH, T). In this calculation, a simplified ion pairing scheme was performed to ensure the ion balance of the input chemical composition following the method in Gysel et al. (2007).

## 2.5 Light extinction coefficient and visibility calculation

Size-resolved chemical composition of the  $\text{NR-PM}_{10}$  from HR-ToF-AMS, mass concentration of equivalent black carbon from MAAP, PNSD data and the H-TDMA-derived liquid water were used to calculate light extinction coefficient (including light absorption and scattering) and visibility degradation of size-resolved particles by the Mie scattering theory described in Barnard et al. (2010). Here, size-resolved equivalent black carbon mass concentration was inferred by the particle mass size distribution measurement from single particle soot photometer in PKUERS. The method of re-distribution of liquid water and HR-ToF-AMS data has been described in the supporting information (Text S1, HR-ToF-AMS introduction section). Thus, with the re-distributed datasets as the input of the Mie scattering theory, the light extinction coefficient for atmospheric particles in the absence and



presence of liquid water with a size range of 100~2500 nm in stokes diameter can be derived. Due to lack of measurements on aerosol particle morphology and mixing state, we assume particles are spherical as described in Barnard et al. (2010). To perform Mie calculation, the complex reflective index of each component is given in Table 1 of Barnard et al. (2010) and references therein. This method shows good agreement with measurements in Mexico City and is consistent as the regional atmospheric chemistry model WRF-Chem. Here, Ext\_550nm\_wet and Ext\_550nm\_dry represent the calculated light extinction coefficient for particles in the presence and absence of liquid water at an incident light wavelength of 550 nm. The corresponding visibility degradation (VIS) for dry/wet particles was calculated from the light extinction coefficient following the Koschmieder equation [6].

$$\text{VIS} = \frac{3.912}{\text{Ext}_{550\text{nm}}} \quad [6]$$

### 3 Results and Discussion

#### 3.1 Nitrate-dominated fine particulate matter pollution

Figure 1 illustrates a summary of chemical composition of NR-PM<sub>1</sub>, ambient RH, size distribution and total aerosol particle liquid water, size distribution and total aerosol surface area concentration during the period of February 29 to March 5, 2016 in the BEST-ONE campaign. During this period, polluted episodes occurred under stagnant meteorological conditions with low wind speed (Figure S6) and elevated ambient RH (Figure 1a). As marked ‘haze period’ in Figure 1, an obvious increase of NR-PM<sub>1</sub> was observed. The secondary inorganic components (sulfate, nitrate and ammonium) were dominant components of the NR-PM<sub>1</sub>, accounting for up to 73% during the ‘haze period’. Particularly, nitrate was



the major contributor of the secondary inorganic components and accounted for up to ~44% of NR-PM<sub>1</sub> mass, while sulfate contributed for ~12% on average.

In the recent decade, severe haze events with high aerosol mass loading occurred frequently in Beijing during wintertime (Hu et al., 2016; Hu et al., 2017; Sun et al., 2014; Sun et al., 2015). To mitigate the air pollution, the Beijing government implemented strict emission controls. The total mass loading of particulate matter has reduced substantially in the recent years (<http://sthjj.beijing.gov.cn/>). With decreasing in PM mass concentration, the mass fraction of particulate nitrate during these haze events in Beijing enhanced substantially. In 2014, the highest fraction of nitrate in PM<sub>1</sub> was reported as ~20% and increased to ~35% in 2016 (Xu et al., 2019b), which is comparable to the ratio (44%) in this study. The particulate nitrate became more dominant in secondary inorganic compounds other than particulate sulfate with the air quality improvement over NCP.

As one of the main hydrophilic compounds in atmospheric aerosol particles, the ability of water uptake at 90% RH of particulate NH<sub>4</sub>NO<sub>3</sub> is comparable with particulate (NH<sub>4</sub>)<sub>2</sub>SO<sub>4</sub> (Kreidenweis and Asa-Awuku, 2014; Wu et al., 2016). However, compared to (NH<sub>4</sub>)<sub>2</sub>SO<sub>4</sub>, NH<sub>4</sub>NO<sub>3</sub> particles have a lower deliquescence RH (62%, 298 K) than (NH<sub>4</sub>)<sub>2</sub>SO<sub>4</sub> (80%, 298 K) (Kreidenweis and Asa-Awuku, 2014), and easily liquify (Li et al., 2017b). In addition, NH<sub>4</sub>NO<sub>3</sub> particles are semi-volatile, the co-condensation of semi-volatile compounds and water (Topping et al., 2013; Hu et al., 2018) could be significant. Therefore, the switching from sulfate-dominated to nitrate-dominated aerosol chemistry may impact on aerosol water uptake. The interaction between aerosol particle liquid water and particulate nitrate formation and visibility degradation should be reconsidered.



### 3.2 Mutual promotion effects between liquid water and nitrate formation

In the following discussion, the high fraction of particulate nitrate during the ‘haze period’ is elucidated by theoretical calculations considering the uptake of  $\text{N}_2\text{O}_5$  and  $\text{HNO}_3$ , and the thermodynamic equilibrium of  $\text{NH}_4\text{NO}_3$ . In particular, the role of aerosol water uptake in particulate nitrate formation is comprehensively investigated.

$\text{N}_2\text{O}_5$  is an important gaseous precursor for nitrate formation via its hydrolysis to form  $\text{HNO}_3$  during nighttime (Brown et al., 2006). Liquid water can enhance aerosol surface areas and volumes, thereby increasing the available heterogeneous reacting medium. Across the development of ‘haze period’, the estimated liquid water increased from  $\sim 1 \mu\text{g}/\text{m}^3$  at the beginning (2<sup>th</sup> March, 14:00~18:00 p.m.) to  $\sim 75 \mu\text{g}/\text{m}^3$  when the haze was fully developed (4<sup>th</sup> March, 4:00~8:00 a.m.). The total surface area and volume concentrations of particles were increased by the liquid water by 2~3% at the beginning and by about 25~40% in the fully-developed haze compared to the ‘dry’ values, respectively (see Figure S7 and S8). Additionally, from the beginning to the fully-developed haze, the uptake coefficient of  $\text{N}_2\text{O}_5$  was enhanced by a factor of 9 from 0.002 to 0.018, and the  $k_{\text{N}_2\text{O}_5}$  increased by a factor of 20 (dry particles); while, considering the increased particle surface area and volume due to water uptake, the respective value of enhanced  $k_{\text{N}_2\text{O}_5}$  was 25 (Figure 2a). Apart from providing extra reacting medium, the abundant liquid water can liquefy the aerosol particles and may reduce any kinetic limitation of mass transfer for reactive gases (Koop et al., 2011; Shiraiwa et al., 2011) and impact thermodynamic equilibrium of semi-volatile compounds (Kulmala et al., 1993; Topping et al., 2013) to contribute to secondary aerosol formation. Our previous study provided the observational evidence that particles may have transitioned from the solid phase to the liquid phase as RH increased from 20% to 60% during



wintertime in Beijing (Liu et al., 2017). In this study, the ambient RH increased from ~10% up to 70% during the haze period, suggesting a likely transition of particles from the solid to liquid phase. Such phase transition may facilitate particulate nitrate formation by increasing diffusion coefficients of dissolved precursors.

To illustrate the facilitation of nitrate formation in the presence of liquid water, we performed the theoretical calculation of equilibrium between particulate  $\text{NH}_4\text{NO}_3$  and gaseous  $\text{HNO}_3$  under dry and ambient conditions, respectively. First, the dissociation constant of  $\text{NH}_4\text{NO}_3$  ( $K_p$ ) was calculated using equation [5] without considering the influence of the liquid water.  $K_p$  ranged from 0.06 (275.3 K) to 4.61 (291.5 K)  $\text{ppb}^2$  during the ‘haze period’. The measured partial pressure product (2.55~9.63  $\text{ppb}^2$ ) was greater than the equilibrium  $K_p$  nearly all the time (Figure 3). In this case, gaseous  $\text{NH}_3$  and  $\text{HNO}_3$  in the atmosphere were supersaturated and would tend to partition into the dry particle phase gradually even in the absence of liquid water. The presence of liquid water under ambient RH can suppress the  $\text{HNO}_3$  equilibrium vapor pressure to nearly zero, changing equilibrium and facilitate the partitioning of nitrate substantially. The equilibrium vapor pressure of  $\text{HNO}_3$  over particles was calculated by E-AIM Model II ([www.aim.env.uea.ac.uk](http://www.aim.env.uea.ac.uk)) taken into account the liquid water. Note that this calculation assumes negligible interaction between dissolved organic components and the activity of  $\text{NO}_3^-$ . In the presence of aerosol associated water, the  $\text{HNO}_3$  equilibrium vapor pressure dropped from its dry values to effectively zero, indicating liquid water significantly favored greater partitioning to particulate nitrate. The negligible equilibrium vapor pressure of  $\text{HNO}_3$  resulted in essentially no  $\text{HNO}_3$  evaporation back to the gas phase and irreversible uptake of  $\text{HNO}_3$  can be assumed under the ambient RH and  $\text{NH}_3$  concentration. This enabled the simplified treatment of the irreversible condensation rate following



Schwartz (1986) used below. As shown in Figure 4, the partitioning ratio (molar ratio between  
320 particulate and total nitrate) increasing with RH was observed during the development of haze, and 98%  
of nitrate was present as particle phase when the haze was fully developed with liquid water increasing  
from  $1 \mu\text{g}/\text{m}^3$  to  $\sim 75 \mu\text{g}/\text{m}^3$ .

Furthermore, the presence of aerosol associated water was substantially enhanced by the uptake rate of  
 $\text{HNO}_3$ , which could dominate the gaseous  $\text{HNO}_3$  partitioning into particle phase throughout the haze  
325 developing. Because the negligible equilibrium vapor pressure suggests that  $\text{HNO}_3$  condensation loss  
was not limited by thermodynamic equilibrium but limited by its uptake rate. The condensation (or  
uptake) rate of  $\text{HNO}_3$  ( $k_{\text{HNO}_3}$ ) can be calculated using equations [3-4]. Here, the lower and upper  
limit of  $k_{\text{HNO}_3}$  were calculated assuming the uptake coefficient ( $\gamma$ ) of  $\text{HNO}_3$  in the range of 0.01 to  
0.5 (Fenter et al., 1994; Leu et al., 1995; Beichert and Finlayson-Pitts, 1996; Abbatt and Waschewsky,  
330 1998; Guimbaud et al., 2002). As shown in Figure 2b and 2c, the lower (upper) limit of  $k_{\text{HNO}_3}$   
increased by a factor of 2.9 (2.7) for dry PNSD and 3.5 (3.1) for wet PNSD from the beginning to fully-  
developed haze period. As one can see, the liquid water facilitated the rate of  $\text{HNO}_3$  uptake and hence  
the particulate nitrate formation.

The above analyses quantify the effect of the increased aerosol surface area and volume concentrations  
335 resulting from the water uptake on the particulate nitrate formation through increased uptake of  $\text{N}_2\text{O}_5$   
and  $\text{HNO}_3$ . Such an effect becomes more pronounced with the increasing pollution throughout the haze  
event owing to the simultaneously increasing ambient RH. Owing to its hygroscopicity, the increased  
ammonium nitrate mass fraction led to a further increase in aerosol surface area and volume





concentrations through additional increase in liquid water, further enhancing uptake of condensable  
340 vapors.

It is worth noting that a similar co-condensation effect between water vapor and semi-volatile organic components (Topping and McFiggans, 2012; Topping et al., 2013; Hu et al., 2018) could promote the haze formation as well, for which there may be some evidence in the current case. Such a co-condensation effect will lead to the enhancement of semi-volatile organic and inorganic (e.g., nitrate)  
345 material with the increasing RH in a developing haze. The associated water will favor partitioning of both particulate nitrate and semi-volatile organic materials to the particle phase depending on the organic solubility, providing a linkage between the development of increasing organic and inorganic particle mass.

### 3.3 The key role of liquid water on visibility degradation

350 Aerosol particles grow up in size as ambient RH increases, further enhances their extinction coefficient and impacts visibility (Zhao et al., 2019; Kuang et al., 2016). In this section, size-resolved extinction coefficient of aerosol particles was estimated, and the influences of liquid water on the extinction coefficient and visibility were quantitatively evaluated. As shown in Figure 5a, the total light extinction coefficient of dry and wet aerosol particles enhanced by a factor of 4.3 and 5.4, respectively, from the  
355 beginning to a fully-developed haze. Correspondingly, the calculated visibility without considering liquid water degraded significantly from ~10 km to less than 2 km within 48 hours during the marked ‘haze period’. The contribution of aerosol associated water to visibility impairment was negligible in the



beginning (2%), while it was significant (up to 24%) in the fully-developed haze (Figure 5b). This indicates that liquid water facilitated visibility degradation during haze development.

360 The influences of liquid water on visibility degradation varied with aerosol particle size. The size-resolved chemical composition data showed that the inorganic species, mainly nitrate, were dominant components in the aerosol particles within the size range of 300~700 nm (Figure S3). Correspondingly, the particles in this size range contained most of the liquid water (50~80% of the total aerosol liquid water content of PM<sub>1</sub>). According to discussion in Sec. 3.2, the mutual promotion effect between liquid  
365 water and particulate nitrate can promote their formation. Aerosol particles in this size range experienced the most significant enhancement of light extinction due to water uptake (Figure 6a and 6b) and contributed 70~88% of the total extinction coefficient of the total NR-PM<sub>1</sub> (Figure S9). In conclude, the rapid nitrate formation enhanced the aerosol extinction coefficient during haze developing, while the aerosol water uptake further enhanced the visibility degradation by increasing  
370 extinction coefficient and promoting nitrate formation.

It is worth noting that the enhanced dimming effect will further shallower the planetary boundary layer (PBL), which, in turn, depresses the dilution of water vapor and particulate matter in the atmosphere, hence leads to a higher RH and aerosol particle mass loading (Tie et al., 2017). Such effect is beyond the scope of this study.



## 375 4 Conclusions and implication

In this study, we observed a nitrate-dominated (up to 44% of non-refractory PM<sub>1</sub> mass concentration) particulate matter pollution episode, which is typical during winter haze in Beijing, China. A clear co-increase of aerosol particle liquid water and particulate nitrate was observed, demonstrating the mutual promotion effect between them via observation-based theoretical calculations.

380 As shown in Figure 7, the water uptake by hygroscopic aerosols increased the aerosol surface area and volume, favoring the thermodynamic equilibrium of ammonium nitrate and enhancing the condensational loss of N<sub>2</sub>O<sub>5</sub> and HNO<sub>3</sub> over particles. The enhanced particulate nitrate formation from the above pathways increased the mass fraction of particulate nitrate, which had a lower deliquescence RH than sulfate and resulted in more water uptake at lower ambient RH (Kreidenweis and Asa-Awuku,  
385 2014). Hence, the increased aerosol particle surface area and volume concentrations due to water uptake, in turn facilitates particulate nitrate formation. Hence, a feedback loop between liquid water and particulate nitrate is built up. Therefore the enhanced particulate nitrate components can accelerate the feedback compared with sulfate-rich pollution over the NCP region in the past (Hu et al., 2016). This self-amplification can rapidly degrade air quality and halve visibility within one day. Our results  
390 highlight the importance of reducing the particulate nitrate and its precursors (e.g. NO<sub>x</sub>) for mitigation of haze episodes in NCP region.



## Data availability

The observational dataset of the BEST-ONE campaign can be accessed through the corresponding author Z. Wu ([zhijunwu@pku.edu.cn](mailto:zhijunwu@pku.edu.cn)).

395 The E-AIM model can be accessed via <http://www.aim.env.uea.ac.uk/aim/aim.php>.

## Author contributions

Z.W., Y.W. and Y.C. conceived the study. Y.Z., M.H., and A.K.S developed BEST-ONE field campaign program. Y.W., Z.W., D.S., Z.D., S.H.S., R.S., G.I.G., P.S., T.H., K.L., L.Z., C.Z., A.K.S., Y.Z., and M.H. participated in this campaign and collected the dataset. Y.W. conducted aerosol particle  
400 liquid water calculation under guide of Y.B. and thermodynamic equilibrium of particulate ammonium nitrate under guidance of G.M. Y.C. calculated the uptake coefficient of  $\text{N}_2\text{O}_5$ , optical properties and visibility. Y.W. and Y.C. cowrite the manuscript with the inputs from all co-authors. Z.W., G.M., A.K.S., S.H.S., G.I.G., P.S., T.H., A.V., and A.W. proofread and help improve the manuscript. All authors discussed the results.

## 405 Acknowledgement

This work is supported by the following projects: National Natural Science Foundation of China (41571130021, 41875149), Ministry of Science and Technology of the People's Republic of China (2016YFC0202801), German Federal Ministry of Education and Research (ID-CLAR). Y.W. acknowledges the support of the China Scholarship Council and The University of Manchester Joint  
410 Scholarship Programme. We thank Dr. Paul I. Williams for valuable advice on reaction constant of  $\text{HNO}_3$  and  $\text{N}_2\text{O}_5$ .



## References

- Abbatt, J. P. D., and Waschewsky, G. C. G.: Heterogeneous Interactions of HOBr, HNO<sub>3</sub>, O<sub>3</sub>, and NO<sub>2</sub> with Deliquescent NaCl Aerosols at Room Temperature, *The Journal of Physical Chemistry A*, 102, 3719-3725, 10.1021/jp980932d, 1998.
- Anttila, T., Kiendler-Scharr, A., Tillmann, R., and Mentel, T. F.: On the Reactive Uptake of Gaseous Compounds by Organic-Coated Aqueous Aerosols: Theoretical Analysis and Application to the Heterogeneous Hydrolysis of N<sub>2</sub>O<sub>5</sub>, *The Journal of Physical Chemistry A*, 110, 10435-10443, 10.1021/jp062403c, 2006.
- Barnard, J. C., Fast, J. D., Paredes-Miranda, G., Arnott, W. P., and Laskin, A.: Technical Note: Evaluation of the WRF-Chem "Aerosol Chemical to Aerosol Optical Properties" Module using data from the MILAGRO campaign, *Atmos. Chem. Phys.*, 10, 7325-7340, 10.5194/acp-10-7325-2010, 2010.
- Beichert, P., and Finlayson-Pitts, B. J.: Knudsen Cell Studies of the Uptake of Gaseous HNO<sub>3</sub> and Other Oxides of Nitrogen on Solid NaCl: The Role of Surface-Adsorbed Water, *The Journal of Physical Chemistry*, 100, 15218-15228, 10.1021/jp960925u, 1996.
- Bian, Y., Zhao, C., Ma, N., Chen, J., and Xu, W.: A study of aerosol liquid water content based on hygroscopicity measurements at high relative humidity in the North China Plain, 6417-6426 pp., 2014.
- Brown, S. S., Ryerson, T. B., Wollny, A. G., Brock, C. A., Peltier, R., Sullivan, A. P., Weber, R. J., Dubé, W. P., Trainer, M., Meagher, J. F., Fehsenfeld, F. C., and Ravishankara, A. R.: Variability in Nocturnal Nitrogen Oxide Processing and Its Role in Regional Air Quality, *Science*, 311, 67-70, 10.1126/science.1120120, 2006.
- Calvert, J. G., Lazrus, A., Kok, G. L., Heikes, B. G., Walega, J. G., Lind, J., and Cantrell, C. A.: Chemical mechanisms of acid generation in the troposphere, *Nature*, 317, 27, 10.1038/317027a0, 1985.
- Chang, W. L., Brown, S. S., Stutz, J., Middlebrook, A. M., Bahreini, R., Wagner, N. L., Dubé, W. P., Pollack, I. B., Ryerson, T. B., and Riemer, N.: Evaluating N<sub>2</sub>O<sub>5</sub> heterogeneous hydrolysis parameterizations for CalNex 2010, *Journal of Geophysical Research: Atmospheres*, 121, 5051-5070, doi:10.1002/2015JD024737, 2016.
- Chen, Y., Wild, O., Wang, Y., Ran, L., Teich, M., Größ, J., Wang, L., Spindler, G., Herrmann, H., van Pinxteren, D., McFiggans, G., and Wiedensohler, A.: The influence of impactor size cut-off shift caused by hygroscopic growth on particulate matter loading and composition measurements, *Atmospheric Environment*, 195, 141-148, https://doi.org/10.1016/j.atmosenv.2018.09.049, 2018a.
- Chen, Y., Wolke, R., Ran, L., Birmili, W., Spindler, G., Schröder, W., Su, H., Cheng, Y., Tegen, I., and Wiedensohler, A.: A parameterization of the heterogeneous hydrolysis of N<sub>2</sub>O<sub>5</sub> for mass-based aerosol models: improvement of particulate nitrate prediction, *Atmos. Chem. Phys.*, 18, 673-689, 10.5194/acp-18-673-2018, 2018b.
- Cheng, Y., Zheng, G., Wei, C., Mu, Q., Zheng, B., Wang, Z., Gao, M., Zhang, Q., He, K., Carmichael, G., Pöschl, U., and Su, H.: Reactive nitrogen chemistry in aerosol water as a source of sulfate during haze events in China, *Science Advances*, 2, 10.1126/sciadv.1601530, 2016.



- Clegg, S. L., Brimblecombe, P., and Wexler, A. S.: Thermodynamic Model of the System  $\text{H}^+ - \text{NH}_4^+ - \text{SO}_4^{2-} - \text{NO}_3^- - \text{H}_2\text{O}$  at Tropospheric Temperatures, *The Journal of Physical Chemistry A*, 102, 2137-2154, 10.1021/jp973042r, 1998.
- de Foy, B., Lu, Z., and Streets, D. G.: Satellite  $\text{NO}_2$  retrievals suggest China has exceeded its  $\text{NO}_x$  reduction goals from the twelfth Five-Year Plan, *Scientific Reports*, 6, 35912, 10.1038/srep35912  
<https://www.nature.com/articles/srep35912#supplementary-information>, 2016.
- DeCarlo, P. F., Kimmel, J. R., Trimborn, A., Northway, M. J., Jayne, J. T., Aiken, A. C., Gonin, M., Fuhrer, K., Horvath, T., Docherty, K. S., Worsnop, D. R., and Jimenez, J. L.: Field-Deployable, High-Resolution, Time-of-Flight Aerosol Mass Spectrometer, *Analytical Chemistry*, 78, 8281-8289, 10.1021/ac061249n, 2006.
- Dong, H. B., Zeng, L. M., Hu, M., Wu, Y. S., Zhang, Y. H., Slanina, J., Zheng, M., Wang, Z. F., and Jansen, R.: Technical Note: The application of an improved gas and aerosol collector for ambient air pollutants in China, *Atmos. Chem. Phys.*, 12, 10519-10533, 10.5194/acp-12-10519-2012, 2012.
- Ervens, B., Turpin, B. J., and Weber, R. J.: Secondary organic aerosol formation in cloud droplets and aqueous particles (aqSOA): a review of laboratory, field and model studies, *Atmos. Chem. Phys.*, 11, 11069-11102, 10.5194/acp-11-11069-2011, 2011.
- Fenter, F. F., Caloz, F., and Rossi, M. J.: Kinetics of Nitric Acid Uptake by Salt, *The Journal of Physical Chemistry*, 98, 9801-9810, 10.1021/j100090a014, 1994.
- Fitzgerald, J. W.: Dependence of the Supersaturation Spectrum of CCN on Aerosol Size Distribution and Composition, *Journal of the Atmospheric Sciences*, 30, 628-634, 10.1175/1520-0469(1973)030<0628:dotso>2.0.co;2, 1973.
- Ge, X., He, Y., Sun, Y., Xu, J., Wang, J., Shen, Y., and Chen, M.: Characteristics and Formation Mechanisms of Fine Particulate Nitrate in Typical Urban Areas in China, *Atmosphere*, 8, 62, 2017.
- Guimbaud, C., Arens, F., Gutzwiller, L., Gäggeler, H. W., and Ammann, M.: Uptake of  $\text{HNO}_3$  to deliquescent sea-salt particles: a study using the short-lived radioactive isotope tracer  $^{13}\text{N}$ , *Atmos. Chem. Phys.*, 2, 249-257, 10.5194/acp-2-249-2002, 2002.
- Guo, S., Hu, M., Zamora, M. L., Peng, J., Shang, D., Zheng, J., Du, Z., Wu, Z., Shao, M., Zeng, L., Molina, M. J., and Zhang, R.: Elucidating severe urban haze formation in China, *Proceedings of the National Academy of Sciences*, 111, 17373-17378, 10.1073/pnas.1419604111, 2014.
- Gysel, M., Crosier, J., Topping, D. O., Whitehead, J. D., Bower, K. N., Cubison, M. J., Williams, P. I., Flynn, M. J., McFiggans, G. B., and Coe, H.: Closure study between chemical composition and hygroscopic growth of aerosol particles during TORCH2, *Atmos. Chem. Phys.*, 7, 6131-6144, 10.5194/acp-7-6131-2007, 2007.
- Gysel, M., McFiggans, G. B., and Coe, H.: Inversion of tandem differential mobility analyser (TDMA) measurements, *Journal of Aerosol Science*, 40, 134-151, <https://doi.org/10.1016/j.jaerosci.2008.07.013>, 2009.



- 485 Heintzenberg, J.: Fine particles in the global troposphere A review, *Tellus B: Chemical and Physical Meteorology*, 41, 149-160, 10.3402/tellusb.v41i2.15064, 1989.
- Hu, D., Topping, D., and McFiggans, G.: Measured particle water uptake enhanced by co-condensing vapours, *Atmos. Chem. Phys.*, 18, 14925-14937, 10.5194/acp-18-14925-2018, 2018.
- 490 Hu, W., Hu, M., Hu, W., Jimenez, J. L., Yuan, B., Chen, W., Wang, M., Wu, Y., Chen, C., Wang, Z., Peng, J., Zeng, L., and Shao, M.: Chemical composition, sources, and aging process of submicron aerosols in Beijing: Contrast between summer and winter, *Journal of Geophysical Research: Atmospheres*, 121, 1955-1977, doi:10.1002/2015JD024020, 2016.
- Hu, W., Hu, M., Hu, W. W., Zheng, J., Chen, C., Wu, Y., and Guo, S.: Seasonal variations in high time-resolved chemical compositions, sources, and evolution of atmospheric submicron aerosols in the  
 495 megacity Beijing, *Atmos. Chem. Phys.*, 17, 9979-10000, 10.5194/acp-17-9979-2017, 2017.
- Huang, R.-J., Zhang, Y., Bozzetti, C., Ho, K.-F., Cao, J.-J., Han, Y., Daellenbach, K. R., Slowik, J. G., Platt, S. M., Canonaco, F., Zotter, P., Wolf, R., Pieber, S. M., Bruns, E. A., Crippa, M., Ciarelli, G., Piazzalunga, A., Schwikowski, M., Abbaszade, G., Schnelle-Kreis, J., Zimmermann, R., An, Z., Szidat, S., Baltensperger, U., Haddad, I. E., and Prévôt, A. S. H.: High secondary aerosol contribution to  
 500 particulate pollution during haze events in China, *Nature*, 514, 218, 10.1038/nature13774  
<https://www.nature.com/articles/nature13774#supplementary-information>, 2014.
- Huang, X. F., He, L. Y., Hu, M., Canagaratna, M. R., Sun, Y., Zhang, Q., Zhu, T., Xue, L., Zeng, L. W., Liu, X. G., Zhang, Y. H., Jayne, J. T., Ng, N. L., and Worsnop, D. R.: Highly time-resolved chemical  
 505 characterization of atmospheric submicron particles during 2008 Beijing Olympic Games using an Aerodyne High-Resolution Aerosol Mass Spectrometer, *Atmos. Chem. Phys.*, 10, 8933-8945, 10.5194/acp-10-8933-2010, 2010.
- Jayne, J. T., Leard, D. C., Zhang, X., Davidovits, P., Smith, K. A., Kolb, C. E., and Worsnop, D. R.: Development of an Aerosol Mass Spectrometer for Size and Composition Analysis of Submicron Particles, *Aerosol Science and Technology*, 33, 49-70, 10.1080/027868200410840, 2000.
- 510 Jimenez, J. L., Jayne, J. T., Shi, Q., Kolb, C. E., Worsnop, D. R., Yourshaw, I., Seinfeld, J. H., Flagan, R. C., Zhang, X., Smith, K. A., Morris, J. W., and Davidovits, P.: Ambient aerosol sampling using the Aerodyne Aerosol Mass Spectrometer, *Journal of Geophysical Research: Atmospheres*, 108, doi:10.1029/2001JD001213, 2003.
- Köhler, H.: The Nucleus in and the Growth of Hygroscopic Droplets., *Transactions of the Faraday Society*, 32, 1152-1161, 1936.
- 515 Kolb, C. E., Cox, R. A., Abbatt, J. P. D., Ammann, M., Davis, E. J., Donaldson, D. J., Garrett, B. C., George, C., Griffiths, P. T., Hanson, D. R., Kulmala, M., McFiggans, G., Pöschl, U., Riipinen, I., Rossi, M. J., Rudich, Y., Wagner, P. E., Winkler, P. M., Worsnop, D. R., and O' Dowd, C. D.: An overview of current issues in the uptake of atmospheric trace gases by aerosols and clouds, *Atmos. Chem. Phys.*, 10, 10561-10605, 10.5194/acp-10-10561-2010, 2010.





- Koop, T., Bookhold, J., Shiraiwa, M., and Poschl, U.: Glass transition and phase state of organic compounds: dependency on molecular properties and implications for secondary organic aerosols in the atmosphere, *Physical Chemistry Chemical Physics*, 13, 19238-19255, 10.1039/C1CP22617G, 2011.
- 525 Kreidenweis, S. M., and Asa-Awuku, A.: 5.13 - Aerosol Hygroscopicity: Particle Water Content and Its Role in Atmospheric Processes A2 - Turekian, Heinrich D. HollandKarl K, in: *Treatise on Geochemistry (Second Edition)*, Elsevier, Oxford, 331-361, 2014.
- Kuang, Y., Zhao, C. S., Ma, N., Liu, H. J., Bian, Y. X., Tao, J. C., and Hu, M.: Deliquescent phenomena of ambient aerosols on the North China Plain, *Geophysical Research Letters*, 43, 8744-8750, doi:10.1002/2016GL070273, 2016.
- 530 Kulmala, M., Laaksonen, A., Korhonen, P., Vesala, T., Ahonen, T., and Barrett, J. C.: The effect of atmospheric nitric acid vapor on cloud condensation nucleus activation, *Journal of Geophysical Research: Atmospheres*, 98, 22949-22958, 10.1029/93JD02070, 1993.
- Leu, M.-T., Timonen, R., F. Keyser, L., and Yung, Y.: Heterogeneous reactions of  $\text{HNO}_3(\text{g}) + \text{NaCl}(\text{s})$  yields  $\text{HCl}(\text{g}) + \text{NaNO}_3(\text{s})$  and  $\text{N}_2\text{O}_5(\text{g}) + \text{NaCl}(\text{s})$  yields  $\text{ClNO}_2(\text{g}) + \text{NaNO}_3(\text{s})$ , 1995.
- 535 Li, C., McLinden, C., Fioletov, V., Krotkov, N., Carn, S., Joiner, J., Streets, D., He, H., Ren, X., Li, Z., and Dickerson, R. R.: India Is Overtaking China as the World's Largest Emitter of Anthropogenic Sulfur Dioxide, *Scientific Reports*, 7, 14304, 10.1038/s41598-017-14639-8, 2017a.
- Li, H., Zhang, Q., Zheng, B., Chen, C., Wu, N., Guo, H., Zhang, Y., Zheng, Y., Li, X., and He, K.: Nitrate-driven urban haze pollution during summertime over the North China Plain, *Atmos. Chem. Phys.*, 18, 5293-5306, 10.5194/acp-18-5293-2018, 2018.
- 540 Li, Y. J., Liu, P. F., Bergoend, C., Bateman, A. P., and Martin, S. T.: Rebounding hygroscopic inorganic aerosol particles: Liquids, gels, and hydrates, *Aerosol Science and Technology*, 51, 388-396, 10.1080/02786826.2016.1263384, 2017b.
- Liu, B. Y. H., Pui, D. Y. H., Whitby, K. T., Kittelson, D. B., Kousaka, Y., and McKenzie, R. L.: The aerosol mobility chromatograph: A new detector for sulfuric acid aerosols, *Atmospheric Environment* (1967), 12, 99-104, https://doi.org/10.1016/0004-6981(78)90192-0, 1978.
- 545 Liu, M., Huang, X., Song, Y., Xu, T., Wang, S., Wu, Z., Hu, M., Zhang, L., Zhang, Q., Pan, Y., Liu, X., and Zhu, T.: Rapid  $\text{SO}_2$  emission reductions significantly increase tropospheric ammonia concentrations over the North China Plain, *Atmos. Chem. Phys.*, 18, 17933-17943, 10.5194/acp-18-17933-2018, 2018.
- 550 Liu, Y., Wu, Z., Wang, Y., Xiao, Y., Gu, F., Zheng, J., Tan, T., Shang, D., Wu, Y., Zeng, L., Hu, M., Bateman, A. P., and Martin, S. T.: Submicrometer Particles Are in the Liquid State during Heavy Haze Episodes in the Urban Atmosphere of Beijing, China, *Environmental Science & Technology Letters*, 4, 427-432, 10.1021/acs.estlett.7b00352, 2017.
- 555 Maitland, G. C., Rigby, M., Smith, E. B., and Wakeham, W. A.: *Intermolecular forces: their origin and determination.*, International series of monographs on chemistry 3, 1981.





- Massling, A., Niedermeier, N., Hennig, T., Fors, E. O., Swietlicki, E., Ehn, M., Hämeri, K., Villani, P., Laj, P., Good, N., McFiggans, G., and Wiedensohler, A.: Results and recommendations from an intercomparison of six Hygroscopicity-TDMA systems, *Atmos. Meas. Tech.*, 4, 485-497, 10.5194/amt-4-485-2011, 2011.
- McFiggans, G., Artaxo, P., Baltensperger, U., Coe, H., Facchini, M. C., Feingold, G., Fuzzi, S., Gysel, M., Laaksonen, A., Lohmann, U., Mentel, T. F., Murphy, D. M., O'Dowd, C. D., Snider, J. R., and Weingartner, E.: The effect of physical and chemical aerosol properties on warm cloud droplet activation, *Atmos. Chem. Phys.*, 6, 2593-2649, 10.5194/acp-6-2593-2006, 2006.
- Middlebrook, A. M., Bahreini, R., Jimenez, J. L., and Canagaratna, M. R.: Evaluation of Composition-Dependent Collection Efficiencies for the Aerodyne Aerosol Mass Spectrometer using Field Data, *Aerosol Science and Technology*, 46, 258-271, 10.1080/02786826.2011.620041, 2012.
- Mozurkewich, M., and Calvert, J. G.: Reaction probability of N<sub>2</sub>O<sub>5</sub> on aqueous aerosols, *Journal of Geophysical Research: Atmospheres*, 93, 15889-15896, doi:10.1029/JD093iD12p15889, 1988.
- Petters, M. D., and Kreidenweis, S. M.: A single parameter representation of hygroscopic growth and cloud condensation nucleus activity, *Atmos. Chem. Phys.*, 7, 1961-1971, 10.5194/acp-7-1961-2007, 2007.
- Petzold, A., and Schönlinner, M.: Multi-angle absorption photometry—a new method for the measurement of aerosol light absorption and atmospheric black carbon, *Journal of Aerosol Science*, 35, 421-441, https://doi.org/10.1016/j.jaerosci.2003.09.005, 2004.
- Petzold, A., Ogren, J. A., Fiebig, M., Laj, P., Li, S. M., Baltensperger, U., Holzer-Popp, T., Kinne, S., Pappalardo, G., Sugimoto, N., Wehrli, C., Wiedensohler, A., and Zhang, X. Y.: Recommendations for reporting "black carbon" measurements, *Atmos. Chem. Phys.*, 13, 8365-8379, 10.5194/acp-13-8365-2013, 2013.
- Pfeifer, S., Müller, T., Weinhold, K., Zikova, N., Martins dos Santos, S., Marinoni, A., Bischof, O. F., Kykal, C., Ries, L., Meinhardt, F., Aalto, P., Mihalopoulos, N., and Wiedensohler, A.: Intercomparison of 15 aerodynamic particle size spectrometers (APS 3321): uncertainties in particle sizing and number size distribution, *Atmos. Meas. Tech.*, 9, 1545-1551, 10.5194/amt-9-1545-2016, 2016.
- Putaud, J.-P., Raes, F., Van Dingenen, R., Brüggemann, E., Facchini, M. C., Decesari, S., Fuzzi, S., Gehrig, R., Hüglin, C., Laj, P., Lorbeer, G., Maenhaut, W., Mihalopoulos, N., Müller, K., Querol, X., Rodriguez, S., Schneider, J., Spindler, G., Brink, H. t., Tørseth, K., and Wiedensohler, A.: A European aerosol phenomenology—2: chemical characteristics of particulate matter at kerbside, urban, rural and background sites in Europe, *Atmospheric Environment*, 38, 2579-2595, https://doi.org/10.1016/j.atmosenv.2004.01.041, 2004.
- Schwartz, S. E.: Mass-Transport Considerations Pertinent to Aqueous Phase Reactions of Gases in Liquid-Water Clouds., *Chemistry of Multiphase Atmospheric Systems*, 6. Springer, Berlin, Heidelberg, 1986.
- Seinfeld, J. H., and Pandis, S. N.: *Atmospheric Chemistry and Physics: from air pollution to climate change*, John Wiley & Sons, INC, 2006.



- 595 Shiraiwa, M., Ammann, M., Koop, T., and Pöschl, U.: Gas uptake and chemical aging of semisolid organic aerosol particles, *Proceedings of the National Academy of Sciences*, 108, 11003-11008, 10.1073/pnas.1103045108, 2011.
- Spindler, G., Müller, K., Brüggemann, E., Gnauk, T., and Herrmann, H.: Long-term size-segregated characterization of PM<sub>10</sub>, PM<sub>2.5</sub>, and PM<sub>1</sub> at the IfT research station Melpitz downwind of Leipzig (Germany) using high and low-volume filter samplers, *Atmospheric Environment*, 38, 5333-5347, <https://doi.org/10.1016/j.atmosenv.2003.12.047>, 2004.
- 600 Sun, Y., Jiang, Q., Wang, Z., Fu, P., Li, J., Yang, T., and Yin, Y.: Investigation of the sources and evolution processes of severe haze pollution in Beijing in January 2013, *Journal of Geophysical Research: Atmospheres*, 119, 4380-4398, 10.1002/2014jd021641, 2014.
- 605 Sun, Y. L., Wang, Z. F., Du, W., Zhang, Q., Wang, Q. Q., Fu, P. Q., Pan, X. L., Li, J., Jayne, J., and Worsnop, D. R.: Long-term real-time measurements of aerosol particle composition in Beijing, China: seasonal variations, meteorological effects, and source analysis, *Atmos. Chem. Phys.*, 15, 10149-10165, 10.5194/acp-15-10149-2015, 2015.
- 610 Swietlicki, E., Hansson, H. C., HäMeri, K., Svenningsson, B., Massling, A., McFiggans, G., McMurry, P. H., PetÄJÄ, T., Tunved, P., Gysel, M., Topping, D., Weingartner, E., Baltensperger, U., Rissler, J., Wiedensohler, A., and Kulmala, M.: Hygroscopic properties of submicrometer atmospheric aerosol particles measured with H-TDMA instruments in various environments—a review, *Tellus B*, 60, 432-469, 10.1111/j.1600-0889.2008.00350.x, 2008.
- 615 Tan, Z., Rohrer, F., Lu, K., Ma, X., Bohn, B., Broch, S., Dong, H., Fuchs, H., Gkatzelis, G. I., Hofzumahaus, A., Holland, F., Li, X., Liu, Y., Liu, Y., Novelli, A., Shao, M., Wang, H., Wu, Y., Zeng, L., Hu, M., Kiendler-Scharr, A., Wahner, A., and Zhang, Y.: Wintertime photochemistry in Beijing: Observations of RO<sub>x</sub> radical concentrations in the North China Plain during the BEST-ONE campaign, *Atmos. Chem. Phys. Discuss.*, 2018, 1-33, 10.5194/acp-2018-359, 2018.
- 620 Tie, X., Huang, R.-J., Cao, J., Zhang, Q., Cheng, Y., Su, H., Chang, D., Pöschl, U., Hoffmann, T., Dusek, U., Li, G., Worsnop, D. R., and O'Dowd, C. D.: Severe Pollution in China Amplified by Atmospheric Moisture, *Scientific Reports*, 7, 15760, 10.1038/s41598-017-15909-1, 2017.
- Topping, D., Connolly, P., and McFiggans, G.: Cloud droplet number enhanced by co-condensation of organic vapours, *Nature Geoscience*, 6, 443, 10.1038/ngeo1809  
<https://www.nature.com/articles/ngeo1809#supplementary-information>, 2013.
- 625 Topping, D. O., and McFiggans, G.: Tight coupling of particle size, number and composition in atmospheric cloud droplet activation, *Atmos. Chem. Phys.*, 12, 3253-3260, 10.5194/acp-12-3253-2012, 2012.
- 630 Wang, G., Zhang, R., Gomez, M. E., Yang, L., Levy Zamora, M., Hu, M., Lin, Y., Peng, J., Guo, S., Meng, J., Li, J., Cheng, C., Hu, T., Ren, Y., Wang, Y., Gao, J., Cao, J., An, Z., Zhou, W., Li, G., Wang, J., Tian, P., Marrero-Ortiz, W., Secrest, J., Du, Z., Zheng, J., Shang, D., Zeng, L., Shao, M., Wang, W., Huang, Y., Wang, Y., Zhu, Y., Li, Y., Hu, J., Pan, B., Cai, L., Cheng, Y., Ji, Y., Zhang, F., Rosenfeld, D., Liss, P. S., Duce, R. A., Kolb, C. E., and Molina, M. J.: Persistent sulfate formation from London



- Fog to Chinese haze, *Proceedings of the National Academy of Sciences*, 113, 13630-13635, 10.1073/pnas.1616540113, 2016.
- 635 Wang, H., Lu, K., Chen, X., Zhu, Q., Chen, Q., Guo, S., Jiang, M., Li, X., Shang, D., Tan, Z., Wu, Y., Wu, Z., Zou, Q., Zheng, Y., Zeng, L., Zhu, T., Hu, M., and Zhang, Y.: High N<sub>2</sub>O<sub>5</sub> Concentrations Observed in Urban Beijing: Implications of a Large Nitrate Formation Pathway, *Environmental Science & Technology Letters*, 4, 416-420, 10.1021/acs.estlett.7b00341, 2017.
- 640 Wang, Y., Zhang, Q. Q., He, K., Zhang, Q., and Chai, L.: Sulfate-nitrate-ammonium aerosols over China: response to 2000–2015 emission changes of sulfur dioxide, nitrogen oxides, and ammonia, *Atmos. Chem. Phys.*, 13, 2635-2652, 10.5194/acp-13-2635-2013, 2013.
- Wang, Y., Wu, Z., Ma, N., Wu, Y., Zeng, L., Zhao, C., and Wiedensohler, A.: Statistical analysis and parameterization of the hygroscopic growth of the sub-micrometer urban background aerosol in Beijing, *Atmospheric Environment*, 175, 184-191, <https://doi.org/10.1016/j.atmosenv.2017.12.003>, 2018.
- 645 Wang, Y., and Chen, Y.: Significant Climate Impact of Highly Hygroscopic Atmospheric Aerosols in Delhi, India, *Geophysical Research Letters*, 0, 10.1029/2019gl082339, 2019.
- Wiedensohler, A., Birmili, W., Nowak, A., Sonntag, A., Weinhold, K., Merkel, M., Wehner, B., Tuch, T., Pfeifer, S., Fiebig, M., Fjåraa, A. M., Asmi, E., Sellegri, K., Depuy, R., Venzac, H., Villani, P., Laj, P., Aalto, P., Ogren, J. A., Swietlicki, E., Williams, P., Roldin, P., Quincey, P., Hüglin, C., Fierz-Schmidhauser, R., Gysel, M., Weingartner, E., Riccobono, F., Santos, S., Gröning, C., Faloon, K., Beddows, D., Harrison, R., Monahan, C., Jennings, S. G., O'Dowd, C. D., Marinoni, A., Horn, H. G., Keck, L., Jiang, J., Scheckman, J., McMurry, P. H., Deng, Z., Zhao, C. S., Moerman, M., Henzing, B., de Leeuw, G., Löschau, G., and Bastian, S.: Mobility particle size spectrometers: harmonization of technical standards and data structure to facilitate high quality long-term observations of atmospheric
- 655 particle number size distributions, *Atmos. Meas. Tech.*, 5, 657-685, 10.5194/amt-5-657-2012, 2012.
- Wu, Z., Hu, M., Lin, P., Liu, S., Wehner, B., and Wiedensohler, A.: Particle number size distribution in the urban atmosphere of Beijing, China, 7967-7980 pp., 2008.
- Wu, Z., Wang, Y., Tan, T., Zhu, Y., Li, M., Shang, D., Wang, H., Lu, K., Guo, S., Zeng, L., and Zhang, Y.: Aerosol Liquid Water Driven by Anthropogenic Inorganic Salts: Implying Its Key Role in Haze
- 660 Formation over the North China Plain, *Environmental Science & Technology Letters*, 5, 160-166, 10.1021/acs.estlett.8b00021, 2018.
- Wu, Z. J., Nowak, A., Poulain, L., Herrmann, H., and Wiedensohler, A.: Hygroscopic behavior of atmospherically relevant water-soluble carboxylic salts and their influence on the water uptake of ammonium sulfate, *Atmos. Chem. Phys.*, 11, 12617-12626, 10.5194/acp-11-12617-2011, 2011.
- 665 Wu, Z. J., Zheng, J., Shang, D. J., Du, Z. F., Wu, Y. S., Zeng, L. M., Wiedensohler, A., and Hu, M.: Particle hygroscopicity and its link to chemical composition in the urban atmosphere of Beijing, China, during summertime, *Atmos. Chem. Phys.*, 16, 1123-1138, 10.5194/acp-16-1123-2016, 2016.
- Xie, Y., Wang, G., Wang, X., Chen, J., Chen, Y., Tang, G., Wang, L., Ge, S., Xue, G., Wang, Y., and Gao, J.: Observation of nitrate dominant PM<sub>2.5</sub> and particle pH elevation in urban Beijing during the
- 670 winter of 2017, *Atmos. Chem. Phys. Discuss.*, 2019, 1-25, 10.5194/acp-2019-541, 2019.



- Xu, Q., Wang, S., Jiang, J., Bhattarai, N., Li, X., Chang, X., Qiu, X., Zheng, M., Hua, Y., and Hao, J.: Nitrate dominates the chemical composition of PM<sub>2.5</sub> during haze event in Beijing, China, *Science of The Total Environment*, 689, 1293-1303, <https://doi.org/10.1016/j.scitotenv.2019.06.294>, 2019a.
- 675 Xu, W., Sun, Y., Wang, Q., Zhao, J., Wang, J., Ge, X., Xie, C., Zhou, W., Du, W., Li, J., Fu, P., Wang, Z., Worsnop, D. R., and Coe, H.: Changes in Aerosol Chemistry From 2014 to 2016 in Winter in Beijing: Insights From High-Resolution Aerosol Mass Spectrometry, *Journal of Geophysical Research: Atmospheres*, 124, 1132-1147, [10.1029/2018jd029245](https://doi.org/10.1029/2018jd029245), 2019b.
- 680 Yu, F., Luo, G.: Simulation of particle size distribution with a global aerosol model: contribution of nucleation to aerosol and CCN number concentrations, *Atmos. Chem. Phys.*, 9, 7691-7710, [10.5194/acp-9-7691-2009](https://doi.org/10.5194/acp-9-7691-2009), 2009.
- Yue, F., Xie, Z., Zhang, P., Song, S., He, P., Liu, C., Wang, L., Yu, X., and Kang, H.: The role of sulfate and its corresponding S(IV)+NO<sub>2</sub> formation pathway during the evolution of haze in Beijing, *Science of The Total Environment*, 687, 741-751, <https://doi.org/10.1016/j.scitotenv.2019.06.096>, 2019.
- 685 Yun, H., Wang, W., Wang, T., Xia, M., Yu, C., Wang, Z., Poon, S. C. N., Yue, D., and Zhou, Y.: Nitrate formation from heterogeneous uptake of dinitrogen pentoxide during a severe winter haze in southern China, *Atmos. Chem. Phys.*, 18, 17515-17527, [10.5194/acp-18-17515-2018](https://doi.org/10.5194/acp-18-17515-2018), 2018.
- Zhang, R., Jing, J., Tao, J., Hsu, S. C., Wang, G., Cao, J., Lee, C. S. L., Zhu, L., Chen, Z., Zhao, Y., and Shen, Z.: Chemical characterization and source apportionment of PM<sub>2.5</sub> in Beijing: seasonal perspective, *Atmos. Chem. Phys.*, 13, 7053-7074, [10.5194/acp-13-7053-2013](https://doi.org/10.5194/acp-13-7053-2013), 2013.
- 690 Zhao, C., Yu, Y., Kuang, Y., Tao, J., and Zhao, G.: Recent Progress of Aerosol Light-scattering Enhancement Factor Studies in China, *Advances in Atmospheric Sciences*, 36, 1015-1026, [10.1007/s00376-019-8248-1](https://doi.org/10.1007/s00376-019-8248-1), 2019.

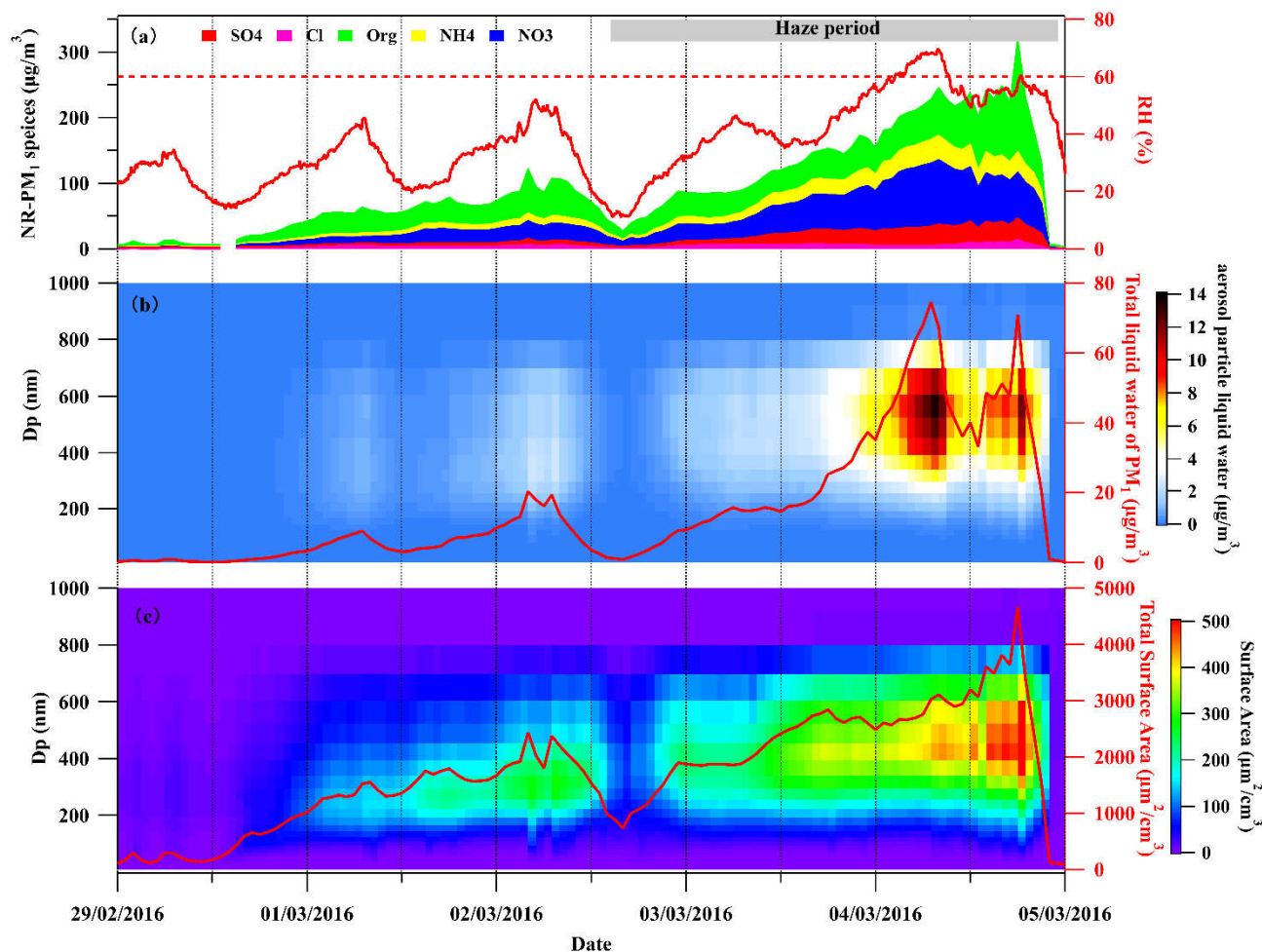


**Figure 1: The time series of (a) NR-PM<sub>1</sub> chemical composition measured by the HR-ToF-AMS and ambient RH (red solid line), (b) size-segregated aerosol particle liquid water and the total mass concentration of liquid water with smaller than 1  $\mu\text{m}$  in aerodynamic diameter (red solid line), (c) size-segregated aerosol particle surface area and total aerosol particle surface area without considering particle hygroscopic growth.**



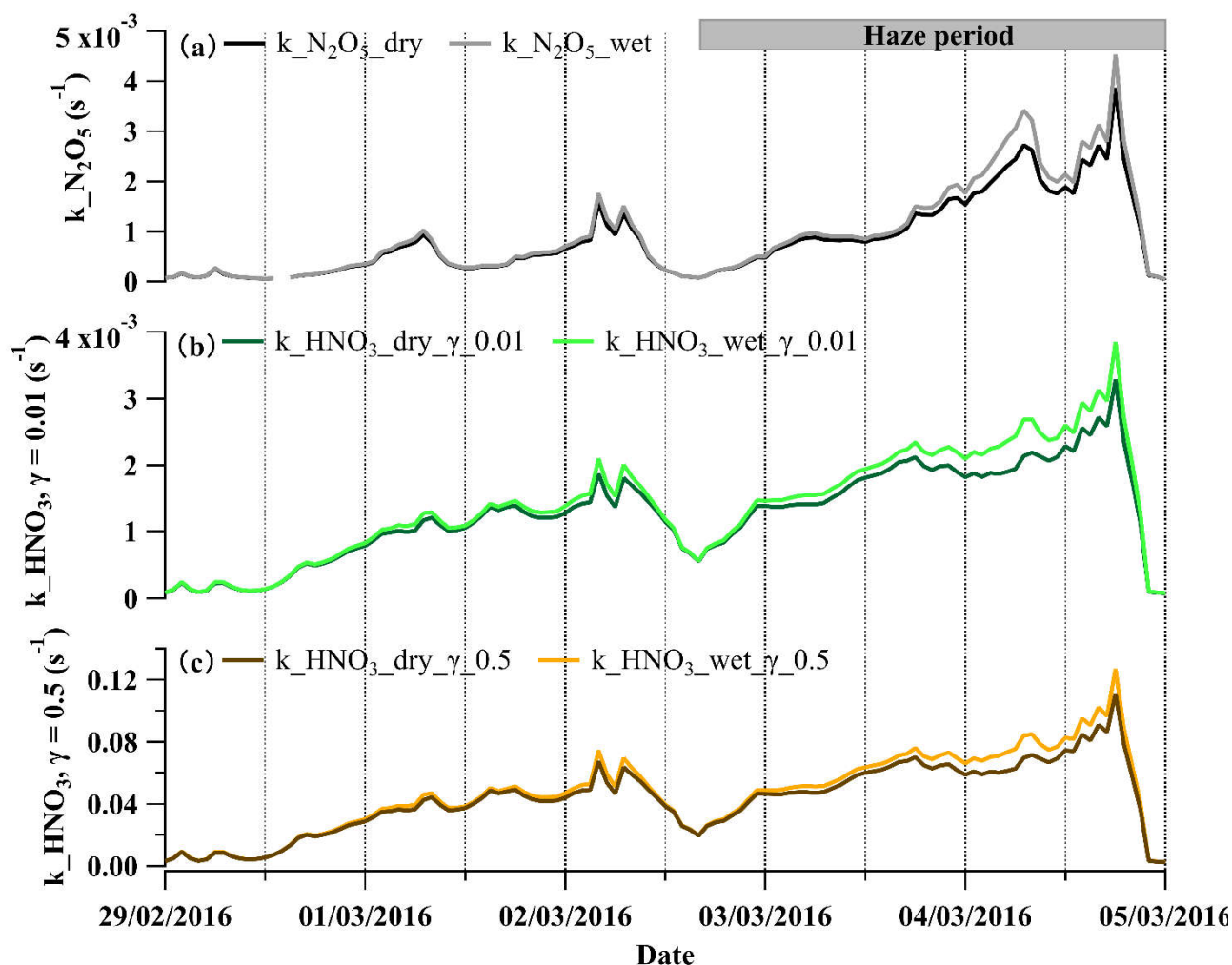


**Figure 2: The time series of (a) condensation rate of  $\text{N}_2\text{O}_5$  ( $k_{\text{N}_2\text{O}_5}$ ) with the calculation of dry particle number size distribution (PNSD) and wet PNSD, (b-c) condensation rate of  $\text{HNO}_3$  ( $k_{\text{HNO}_3}$ ) with the calculation of dry and wet PNSD under the assumption of  $\gamma=0.01$  and  $\gamma=0.5$ , respectively during February 29 to March 5, 2016.**

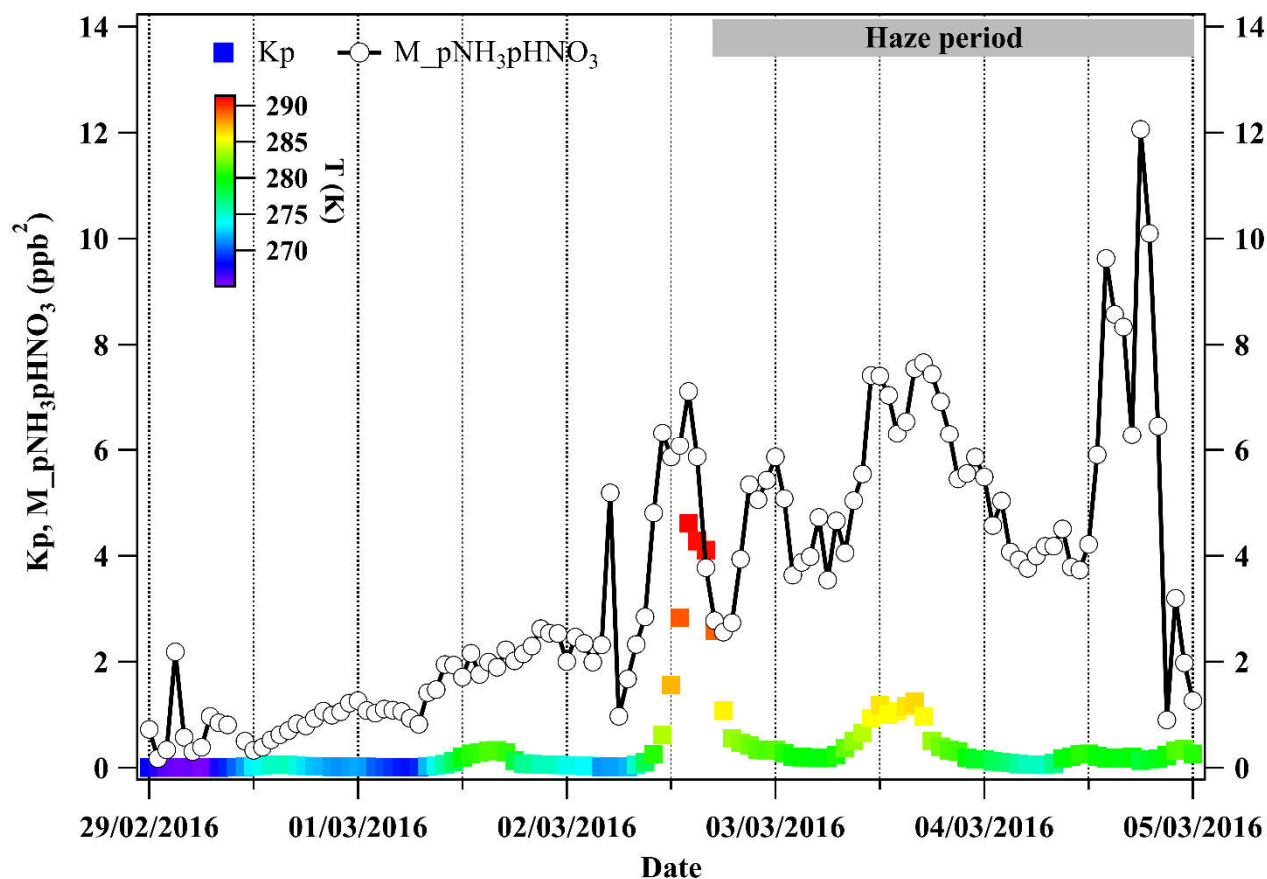


**Figure 3:** The comparison of the calculated temperature-dependent dissociation constant of  $\text{NH}_4\text{NO}_3$  ( $K_p$ ) (Seinfeld. and Pandis., 2006) in the absence of liquid water and the product of mixing ratios of gaseous  $\text{NH}_3$  and  $\text{HNO}_3$  measured by GAC-IC ( $M_{\text{pNH}_3\text{pHNO}_3}$ ). Here,  $K_p$  is colored by the ambient temperature ranging 265~293K during February 29 to March 5, 2016.

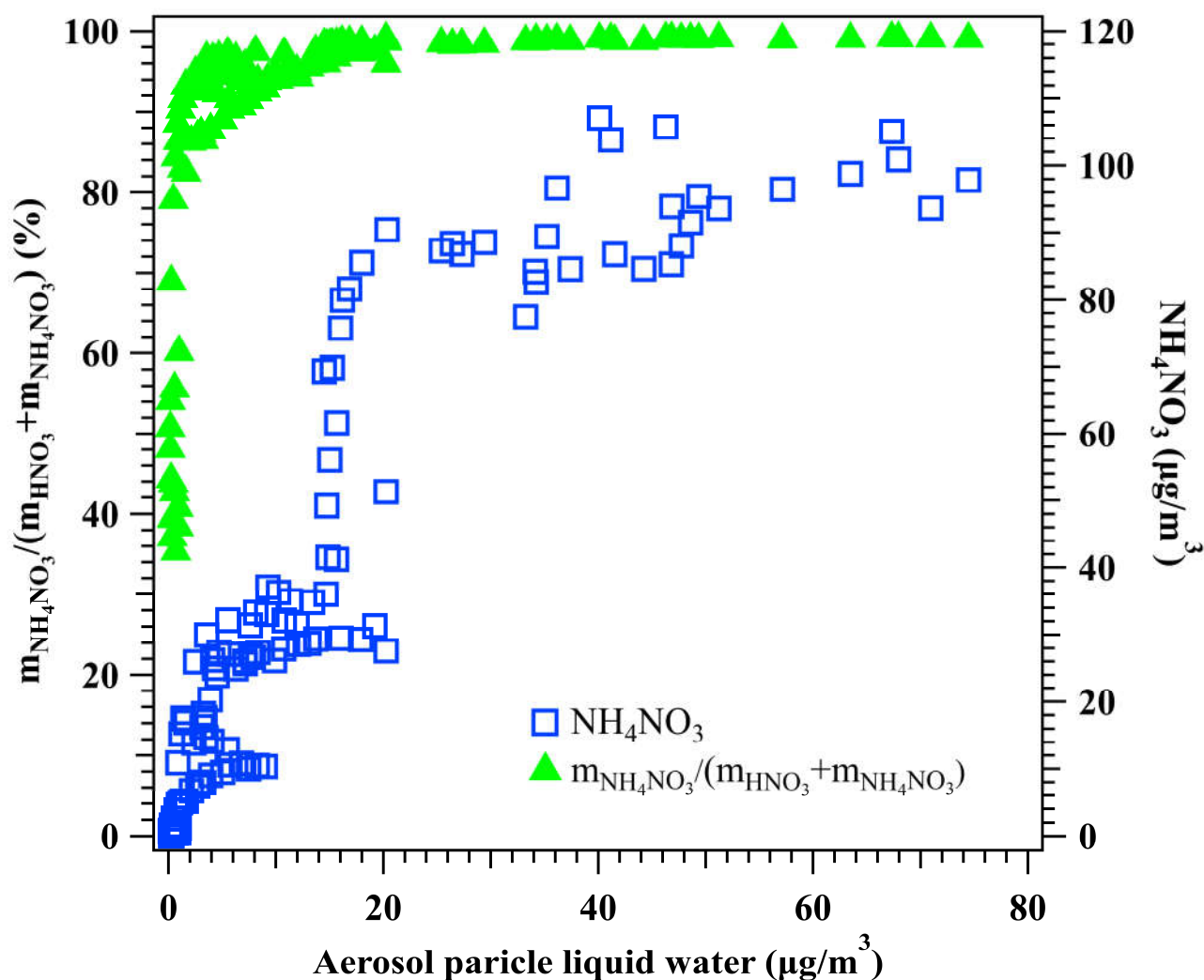
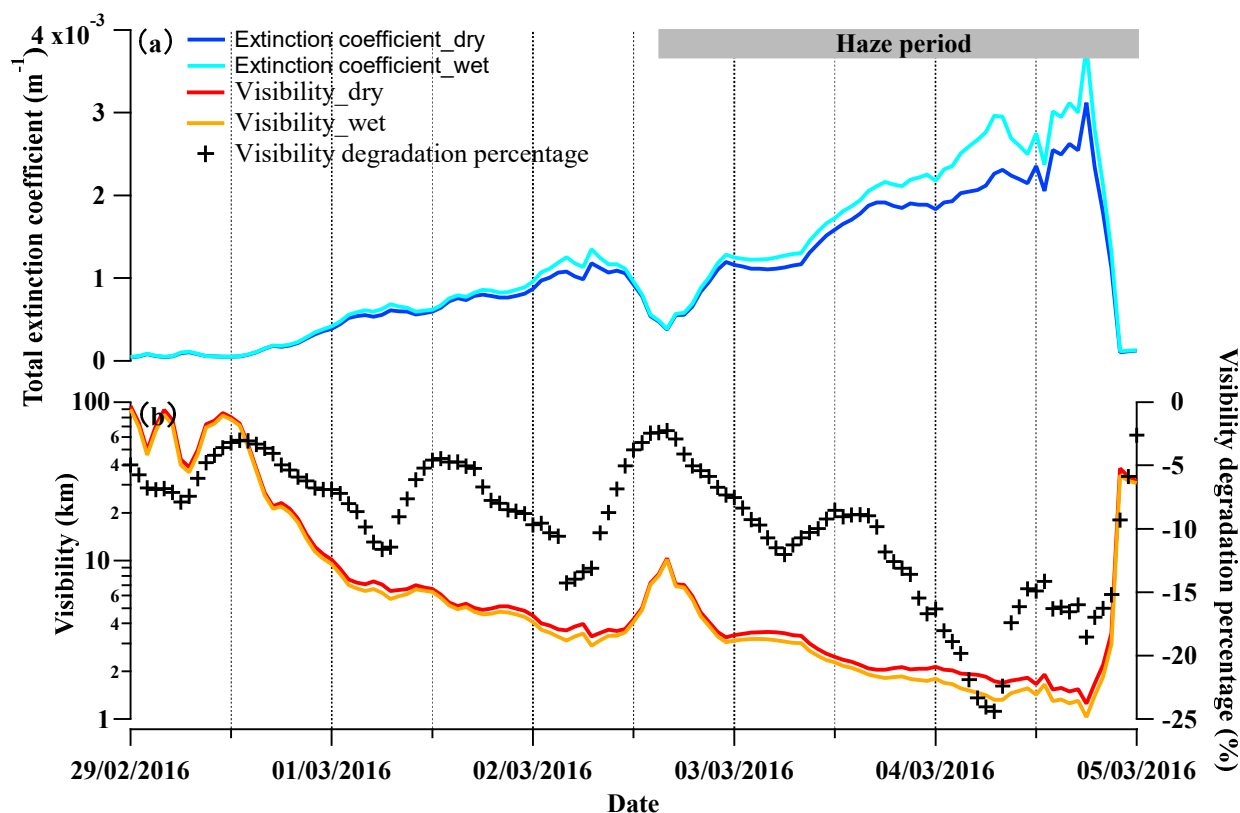
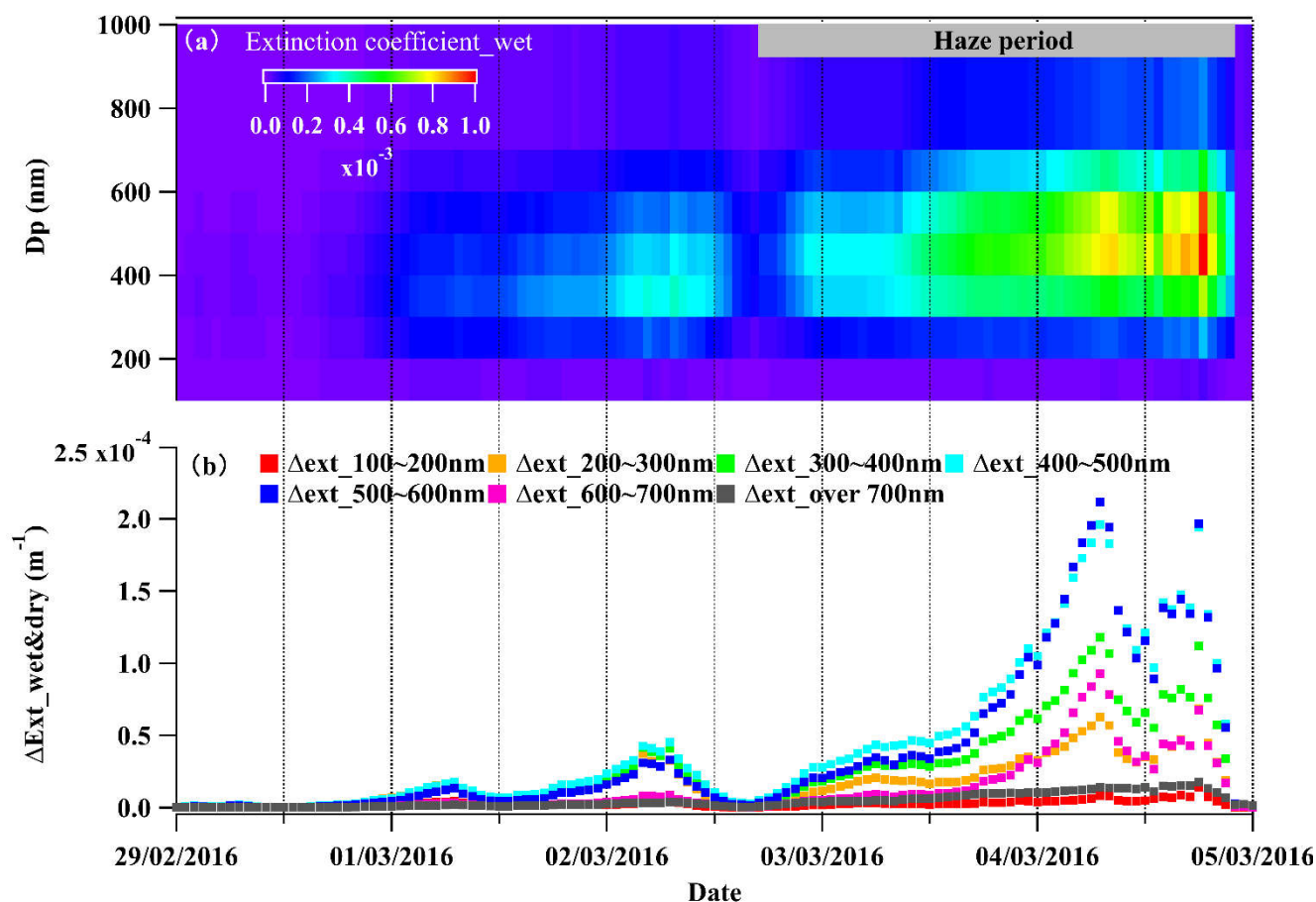


Figure 4: The relationship between aerosol particle liquid water and  $m_{\text{NH}_4\text{NO}_3}/(m_{\text{HNO}_3} + m_{\text{NH}_4\text{NO}_3})$  (left axis) and mass concentration of  $\text{NH}_4\text{NO}_3$  in the particle phase (right axis) during the period of February 29 to March 5, 2016. Here,  $\text{NH}_4\text{NO}_3$  in the particle phase was measured by HR-ToF-AMS and the  $\text{HNO}_3$  in the gas phase was measured by GAC-IC. Liquid water was calculated by H-TDMA-derived method.





720 **Figure 5:** The time series of (a) calculated total extinction coefficient at wavelength of 550 nm with  
 the consideration of dry and wet PNSD, referred as Extinction coefficient\_dry and Extinction  
 coefficient\_wet, (b) calculated visibility with the consideration of dry and wet PNSD, referred as  
 Visibility\_dry and Visibility\_wet, respectively. Visibility degradation percentage is  
 (Visibility\_wet-Visibility\_dry)/Visibility\_dry, representing the visibility degradation in the  
 725 presence of liquid water.



**Figure 6: (a) Size-segregated light extinction coefficient at wavelength of 550 nm for wet particles (Extinction coefficient\_wet), (b) size-segregated difference between Extinction coefficient\_wet and Extinction coefficient\_dry, representing light extinction coefficient difference with and without considering liquid water.**

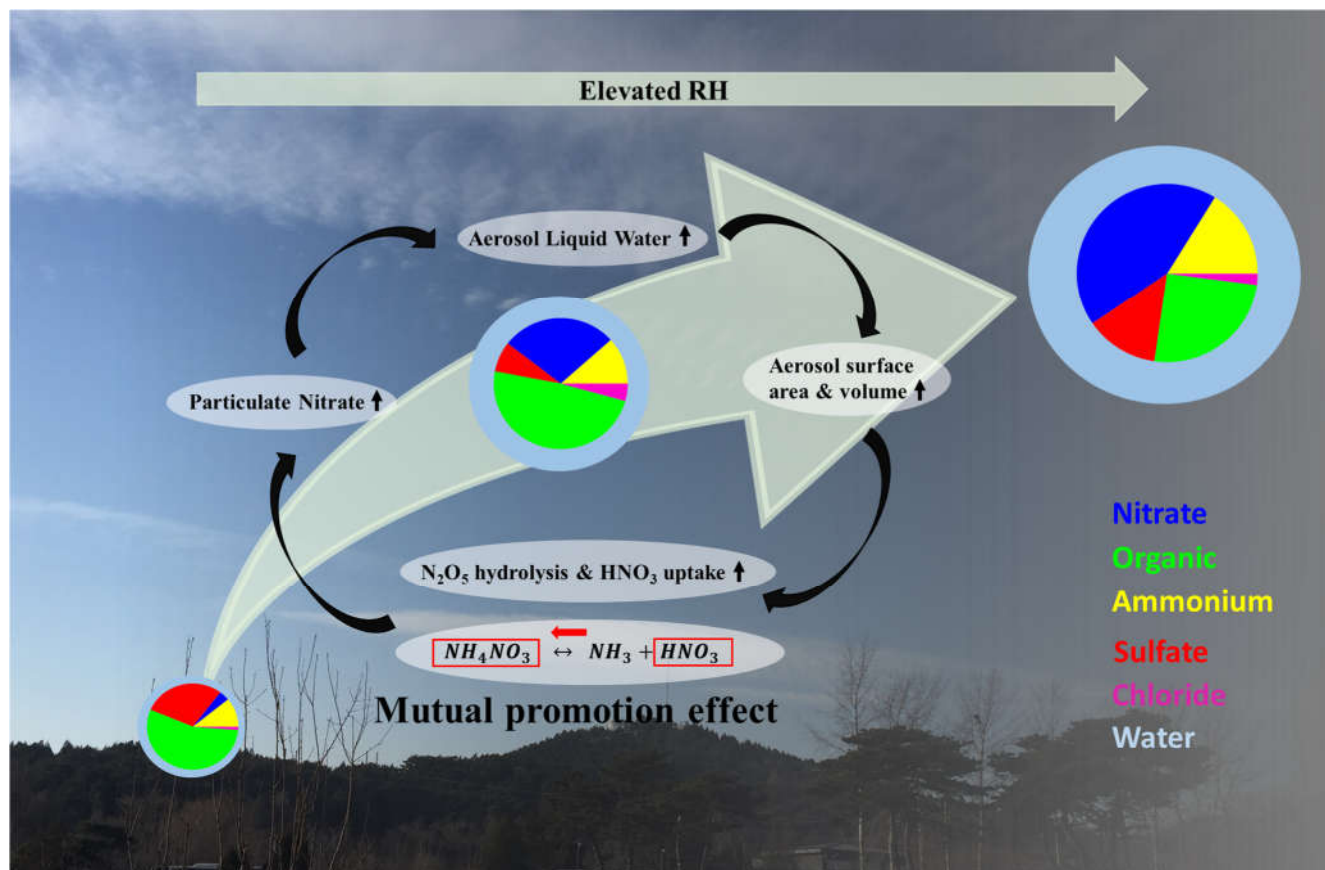


**Figure 7: The scheme of the mutual promotion effect between aerosol liquid water and particulate nitrate**

735

740